Development 139, 4291 (2012) doi:10.1242/dev.090324

Mechanism of pectoral fin outgrowth in zebrafish development

Tohru Yano, Gembu Abe, Hitoshi Yokoyama, Koichi Kawakami and Koji Tamura

There was an error published in *Development* **139**, 2916-2925.

The last reference in the list was truncated. It should read:

Zhang, J., Wagh, P., Guay, D., Sanchez-Pulido, L., Padhi, B. K., Korzh, V., Andrade-Navarro, M. A. and Akimenko, M. A. (2010). Loss of fish actinotrichia proteins and the fin-to-limb transition. *Nature* **466**, 234-237.

We apologise to the authors and readers for this mistake.

Development 139, 2916-2925 (2012) doi:10.1242/dev.075572

Mechanism of pectoral fin outgrowth in zebrafish development

Tohru Yano[1], Gembu Abe[2], Hitoshi Yokoyama[1], Koichi Kawakami[2,3] and Koji Tamura[1,*]

SUMMARY

Fins and limbs, which are considered to be homologous paired vertebrate appendages, have obvious morphological differences that arise during development. One major difference in their development is that the AER (apical ectodermal ridge), which organizes fin/limb development, transitions into a different, elongated organizing structure in the fin bud, the AF (apical fold). Although the role of AER in limb development has been clarified in many studies, little is known about the role of AF in fin development. Here, we investigated AF-driven morphogenesis in the pectoral fin of zebrafish. After the AER-AF transition at ~36 hours post-fertilization, the AF was identifiable distal to the circumferential blood vessel of the fin bud. Moreover, the AF was divisible into two regions: the proximal AF (pAF) and the distal AF (dAF). Removing the AF caused the AER and a new AF to re-form. Interestingly, repeatedly removing the AF led to excessive elongation of the fin mesenchyme, suggesting that prolonged exposure to AER signals results in elongation of mesenchyme region for endoskeleton. Removal of the dAF affected outgrowth of the pAF region, suggesting that dAF signals act on the pAF. We also found that the elongation of the AF was caused by morphological changes in ectodermal cells. Our results suggest that the timing of the AER-AF transition mediates the differences between fins and limbs, and that the acquisition of a mechanism to maintain the AER was a crucial evolutionary step in the development of tetrapod limbs.

KEY WORDS: Fin development, Fin-to-limb, Evolution, Zebrafish

INTRODUCTION

The paired pectoral and pelvic fins of teleost fish contain two different bone elements. Endoskeletal elements are formed as chondral bone through endochondral ossification; exoskeletal elements (fin rays) are formed by intramembranous ossification (Hall, 2005). Fin rays are unique to, and common in, the fins of actinopterygians (e.g. teleosts) and basal sarcopterygians (e.g. coelacanths and lung fish), but this structure is never seen in tetrapod limbs. Nevertheless, fins and limbs are thought to be homologous organs, as they have similar developmental mechanisms, and fossil records are consistent with this idea (Shubin et al., 2006; Mercader, 2007; Boisvert et al., 2008). The endoskeletal elements proximal to fin rays in the teleost pectoral fin are poorly patterned along the proximodistal (PD) axis, whereas limb endoskeletal elements exhibit a well-organized sequential pattern (stylopod, zeugopod and autopod) (Tamura et al., 2008). Many studies suggest that fin structures transformed into limbs by changes in genetic and developmental programs during tetrapod evolution (Sordino et al., 1995; Metscher et al., 2005; Ahn and Ho, 2008; Yonei-Tamura et al., 2008; Sakamoto et al., 2009; Woltering and Duboule, 2010).

Limb evolution involved both better endoskeletal element patterning and the elimination of fin rays. In teleost paired-fin development, the epithelial tissue covering the fin ray region derives from an elongated epidermal structure, the apical fold (AF), which does not form in developing limbs (Dane and Tucker, 1985; Thorogood, 1991). In early paired-fin development, the apical ectodermal ridge (AER) rims the distal edge of the fin bud along the dorsoventral boundary and promotes cell proliferation and mesenchyme outgrowth, which differentiates into endoskeletal elements as seen in limb development (Grandel and Schulte-Merker, 1998; Grandel et al., 2000; Kawakami et al., 2003). Although the limb AER persists until the end of the digit-patterning stage (Mariani and Martin, 2003), and disappears when patterning of the most distal endoskeletal element (the distal phalanx) ceases, the fin AER transforms into an extended structure, the AF, from the middle stage of fin development (Dane and Tucker, 1985).

As the AF elongates distally, migrating mesenchymal cells invade a slit between the AF layers, and two rows of actinotrichia (pre-fin-ray fibers) are formed in this subepidermal space, followed by the formation of lepidotrichia (bony fin-ray segments) (Wood and Thorogood, 1984; Dane and Tucker, 1985; Zhang et al., 2010). With the exception of histological descriptions, however, the AF structure has been poorly characterized, and its function in fin development is still unclear. Analyses of mutants or morphants that affect the function of AER/AF marker genes have indeed shown pectoral fin loss (Grandel et al., 2000; Fischer et al., 2003; Kawakami et al., 2004), but those analyses have not distinguished AF functions from AER functions. Nevertheless, one model of limb evolution, the clock model (supplementary material Fig. S1), suggests that a heterochronic shift of the transformation from AER to AF determined the evolutional fin-to-limb transition (Thorogood, 1991). In this model, the AER-AF transformation occurs early in teleost fin development, later in sarcopterygian fin development, and never in tetrapod limb development. However, little embryological evidence that would test this intriguing hypothesis has been reported.

In this study, we investigated the timing of the AER-to-AF transformation, the structure of the AF, and differential gene expression in the AF in detail. Moreover, we obtained experimental embryological data on the function of the AER and the AF in

[1]Department of Developmental Biology and Neurosciences, Graduate School of Life Sciences, Tohoku University, Aobayama Aoba-ku, Sendai 980-8578, Japan. [2]Division of Molecular and Developmental Biology, National Institute of Genetics. [3]Department of Genetics, The Graduate University for Advanced Studies (SOKENDAI), Mishima, Shizuoka 411-8540, Japan.

*Author for correspondence (tam@m.tohoku.ac.jp)

Accepted 31 May 2012

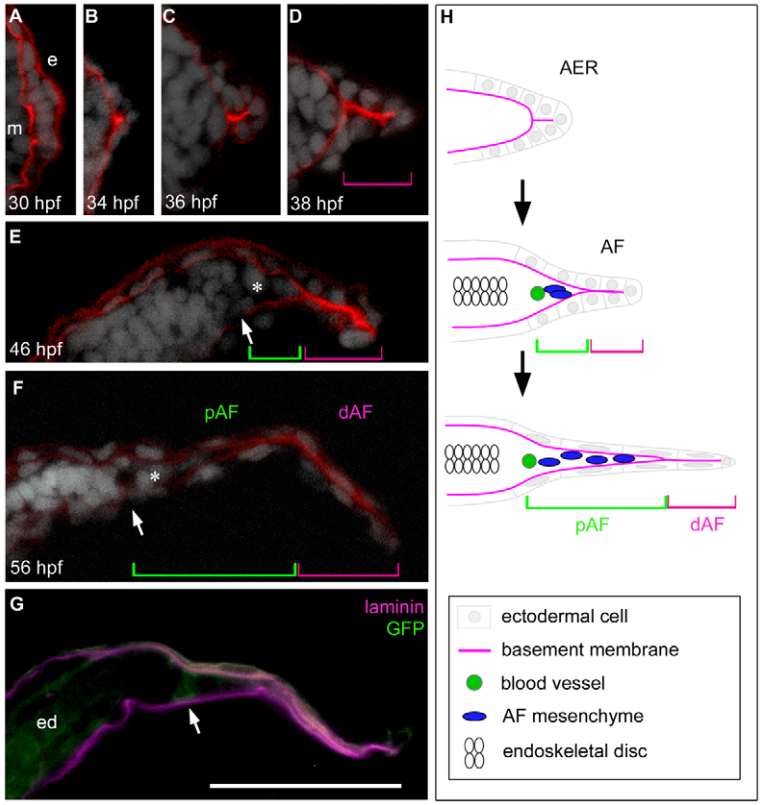

Fig. 1. AER-AF transition and morphological features in pectoral fin development. (**A-G**) A series of transverse pectoral fin bud sections (distal is to the right and dorsal is to the top) at the indicated stages. The basement membrane (red), shown by Laminin α5 immunostaining, is located between the ectoderm (e) and mesoderm (m) (A). Cell nuclei are visualized by DAPI (white). The distal portion of the AF (magenta brackets) consists of ectodermal cells only, and mesenchymal cells (asterisks) enter the notch of the AF within the proximal AF region (green brackets). The circumferential fin blood vessel (white arrows) is located at the base of the AF (E-G), and is recognizable by GFP distribution in *fli1*:EGFP y1 transgenic fish (G). ed, endoskeletal disc. Scale bar: 50 μm. (**H**) Diagram of transverse fin bud sections during AER/AF morphogenesis.

endoskeletal and fin ray development that support the clock model. We also found that changes in ectodermal cell shape are important for AF outgrowth at later stages of development.

MATERIALS AND METHODS

Fish stock, maintenance, staging and fin observation

Adult zebrafish (*Danio rerio*) were maintained at 27°C. Embryos obtained by natural crossing were staged by a standard method (Kimmel et al., 1995), and were raised at 28.5°C until the appropriate stages. Excised pectoral fins and fin buds were put on glass slides filled with Tyrode's solution under coverslips, and analyzed under a BX51 microscope, a DP72 microscope with e-tiling systems (Olympus) and TCS-SP5 confocal microscope (Leica).

Immunochemistry and in situ hybridization

Embryos were fixed in 4% paraformaldehyde (PFA) in PBS for 10 hours at 4°C, then either dehydrated for preparing paraffin-embedded sections or put into gelatin-embedded solution [gelatin (Sigma, G7041):30% sucrose:DDW=3:2:1] for preparing gelatin-frozen sections, which is a more delicate and sensitive technique than other sectioning methods (Fagotto and Gumbiner, 1994; Suzuki et al., 2010). Immunochemistry was performed as described previously (Nechiporuk and Keating, 2002). The following primary antibodies were used: anti-Laminin α5 rabbit IgG (Sigma), 1:200; anti-GFP rat IgG (Sigma), 1:500; and anti-BrdU mouse IgG, 1:100. The species-specific secondary antibodies used were Alexa 488 or 594 (Molecular Probes). Whole-mount and section in situ hybridizations were performed as described previously (Abe et al., 2007). RNA probes were synthesized with the following cDNA fragments: *dlx5a* (a kind gift from Dr Atsushi Kawakami, Tokyo Institute of Technology, Japan), *fgf10a* (a kind gift from Dr Akira Kudo, Tokyo Institute of Technology, Japan), *fgf24* (a kind gift from Dr Kyo Yamasu, Saitama University, Japan), *apoE* [an 800-bp fragment isolated with the primers 5′-CAGCTCAGCAGRGARCTNGA-3′ and 5′-GTCTCCTTNACRTTRTCCAT-3′ using RT-PCR on 24 hours post-fertilization (hpf) embryo RNA] and *predicted rspo2* (a 989-bp fragment isolated from the A8DZD0_DANRE gene with the primers 5′-CCAAG-CTCTTCCTGTTCCTG-3′ and 5′-CGTGGAGAAAGGCAATTCAT-3′ using RT-PCR on 24 hpf embryo RNA). For genotype analyses of the HG21C mutant by PCR, genome DNA was eluted from samples after in situ hybridization and amplified by tcf7-f2/tcf7-r2 primers and by ef1a-f/ef1a-r primers for control PCR (Nagayoshi et al., 2008). For bromodeoxyuridine (BrdU) treatment, samples were incubated in BrdU solution (10 mM BrdU and 15% DMSO) for 15 minutes on ice followed by 1 hour at 28.5°C prior to fixation. All staining and observations were repeated, yielding equivalent results ($n \geq 5$). We show a typical specimen in each figure in the Results section.

Removal experiments and skeletal staining

Fish embryos were anesthetized and immersed in tricaine solution and 2% methylcellulose in fish water. Fin epidermis was mechanically removed with a fine glass-capillary needle. After excision, the embryos were placed in E2 buffer for 30 minutes and incubated in fish water at 28.5°C. For repeated AF removal, the excision was performed at intervals of one to two days. For skeletal analysis of the manipulated fins, Alcian Blue and Alizarin Red staining was performed as described previously (Grandel and Schulte-Merker, 1998).

Inhibitor treatment

Fish embryos were incubated in 0.3 M LiCl in fish water (Joly et al., 1993) for a maximum of 2 hours at room temperature. Control embryos were exposed to 0.3 M NaCl in fish water. During the treatment, time-lapse fluorescence images were taken with a Leica FW4000 every 15 minutes. After the treatment, samples were fixed in 4% PFA in PBS for 2 hours and stained for F-actin using phalloidin Alexa 594 (Invitrogen). Samples were analyzed under an FV1000 confocal microscope (Olympus) and a TCS-SP5 confocal microscope.

RESULTS

Histological observations showing timing of the AER-to-AF transition and structure of the AF

Immunostaining of Laminin α5, which accumulates in the basement membrane under the ectoderm (Webb et al., 2007), enabled us to distinguish the AF from the AER during pectoral fin development in zebrafish (Fig. 1). At 30 hpf, the distal apex

of the epidermis surrounding the mesenchyme was thickened, and the thickened epidermis existed as a single layer (Fig. 1A), a typical morphological trait of the AER. By 34 hpf, the AER had formed a small notch where two sheets of epidermis approached each other (Fig. 1B), a structure also seen in the avian AER (Todt and Fallon, 1984). At 36 and 38 hpf, the notch started to extend and make a slit, dividing the two epithelial layers. This distinctive morphological change marks the transformation of the AER into the AF (Fig. 1C,D). By 46 hpf, the distal fin mesenchyme had started migrating into the base of the AF, and continued to invade distally in a slit between the two layers of the AF (Fig. 1E,F, asterisks). At 56 hpf, there were two portions to the AF: a distal region containing no mesenchyme (distal AF, dAF) and a proximal region with migrating mesenchyme (proximal AF, pAF) (Fig. 1F). The mesenchymal cell migration, however, made it difficult for us to distinguish the proximal border of the pAF (Fig. 1E,F).

We noticed that a blood vessel formed a stable landmark of the border between the AF and non-AF regions (i.e. fin ray and endoskeletal regions) (Fig. 1E,F, arrows), and we used *fli1*:EGFP y1 transgenic fish (Isogai et al., 2001; Lawson and Weinstein, 2002), which enabled us to visualize endothelial cells in blood vessels and endochondral cells in the endoskeletal region of the paired fins (Fig. 1G,H). In the pectoral fin bud, blood vessels invade from anterior and posterior sides at ~43 hpf (Fig. 2A), emigrate peripherally, and are connected at the posterior portion of the bud at ~48 hpf (Fig. 2B). The circumferential blood vessel loop divided the fin bud into endoskeletal and AF regions (Fig. 2C), and the mesenchyme region for the endoskeleton was always inside the circumferential blood vessel loop (Fig. 1G, Fig. 2D-G). The AF can be therefore defined as the epithelial structure distal to the circumferential fin blood vessel. This definition enabled us to further divide the AF into two regions: dAF and pAF (Fig. 1H, see also Fig. 9). The dAF consists only of epidermis. The pAF has two epidermal cell layers separated by a split into which mesenchymal cells migrate; its proximal border is at the circumferential fin blood vessel. The AF epidermal cell nuclei were markedly flattened (Fig. 1F,G), as described previously (Dane and Tucker, 1985).

Spatiotemporal pectoral fin shape changes

Using the circumferential fin blood vessel as a reliable landmark, we observed the spatiotemporal fin shape changes, focusing on AF morphogenesis. The PD length of the endoskeletal region increased continuously but mildly after AF formation (Fig. 2D-G). The AF region grew more rapidly than the endoskeletal region until ~60 hpf (Fig. 2H). These observations revealed that in pectoral fin morphogenesis, elongation of the AF region after the AER-AF transition mainly contributes to fin outgrowth.

To visualize the distal AF compartment, we took advantage of Tol2 enhancer trap constructs (Asakawa et al., 2008; Nagayoshi et al., 2008) in genetic screens, and found that the hspGFFDMC131A line expressed Gal4FF, as visualized by UAS:GFP reporter gene expression, in the distal epidermis in the pectoral fin bud AF (Fig. 3). This line harbored a *Tol2*-transposon insertion, hspGFFDMC enhancer trap construct, neighboring the *R-spondin2* (*rspo2*, ENSDARG00000079570) gene (Fig. 3A). *Rspo2* in amniotes is expressed in the AER (Nam et al., 2007; Aoki et al., 2008). In the hspGFFDMC131A;UAS:GFP line, GFP fluorescence was distributed at the edge of the AF (Fig. 3B) as well as in the brain, branchial arch and spinal cord, and at the AER and the edge of the median fin fold (MFF) (supplementary material Fig. S2). The *rspo2* gene was expressed at the pectoral fin bud in a similar pattern (supplementary material Fig. S3). To examine whether the GFP (*rspo2*)-expressing region corresponds to the dAF, we crossed hspGFFDMC131A;UAS:GFP fish with the *fli1*:EGFP transgenic line. We found that GFP-positive epidermal cells in hspGFFDMC131A;UAS:GFP fish were located far from the circumferential fin blood vessel (Fig. 3C). The pAF was GFP-negative, indicating that the GFP-positive cells in the hspGFFDMC131A;UAS:GFP fish were dAF epidermal cells. Analysis of GFP expression in the pectoral fin over time confirmed that the AF region, a GFP-negative space for the pAF in particular, continued to extend considerably (Fig. 3D-H). Detailed observation of cell shape revealed that morphology of ectodermal cells in both the dAF (Fig. 3I,J) and the pAF (Fig. 1F,H) changes from spindle-shaped and slender (Fig. 3I′) to thin, flat and polygonal (Fig. 3J′).

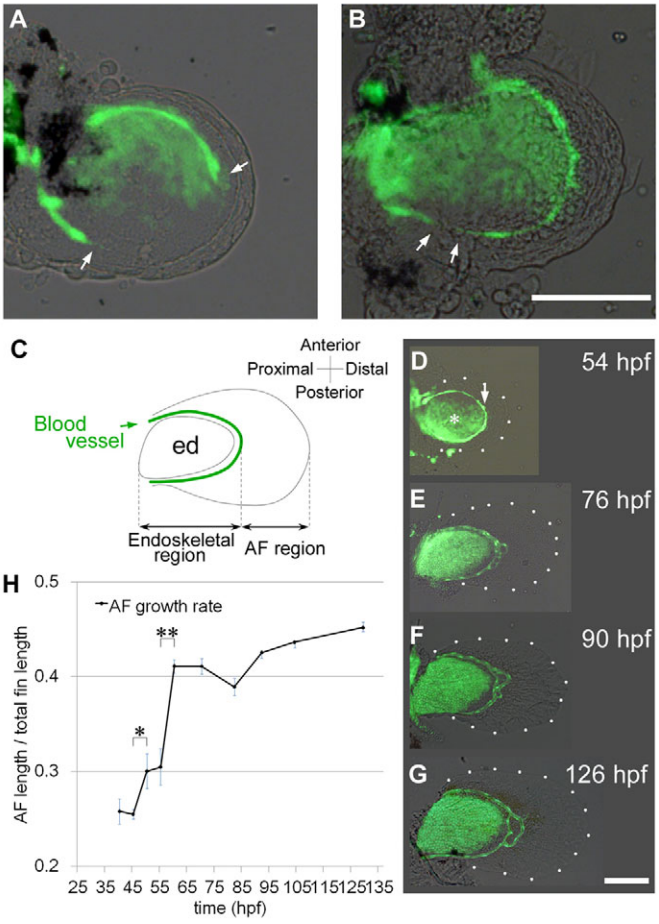

Fig. 2. Pectoral fin outgrowth after the AER-AF transition. (**A**,**B**) *fli1*:EGFP y1 fish fin at 43 (A) and 48 (B) hpf, showing developing circumferential fin blood vessel (white arrows). (**C**) Schematic of a pectoral fin bud. ed, endoskeletal disc. (**D-G**) Whole-mount observation of pectoral fin bud outgrowth at the indicated stages. GFP (green) was distributed in the circumferential blood vessel (white arrow) and the endoskeletal disc (asterisk). White dots indicate the fin margin. (**H**) Temporal changes in AF and endoskeletal region lengths (see also supplementary material Table S1). Error bars indicate s.e.m. AF growth rate (ratio of AF length to total length of the pectoral fin) increased most rapidly until ~60 hpf (data were analyzed by Student's *t*-test; **P*<0.05; ***P*<0.001). Scale bars: 100 μm.

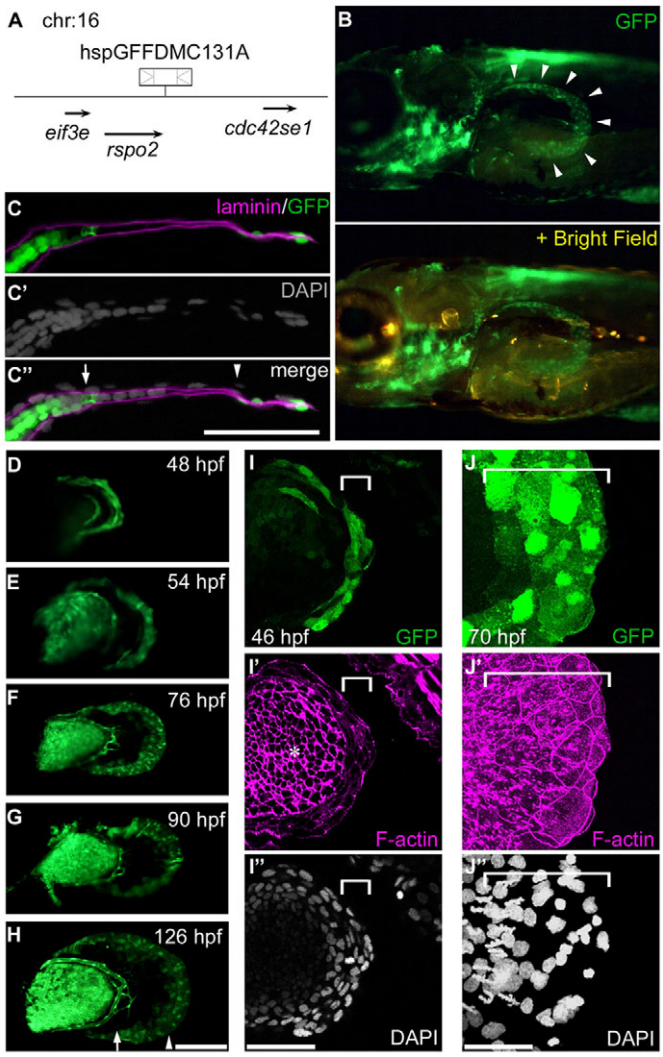

Fig. 3. GFP distribution within the distal AF in the hspGFFDMC131A;UAS:GFP line. (**A**) The hspGFFDMC131A insertion is located 6.6 kb downstream of the *R-spondin 2* (*rspo2*) gene on chromosome 16. (**B**) An hspGFFDMC131A embryo crossed with the UAS:GFP line. The panel is a lateral view of the pectoral fin bud at 76 hpf; the GFP-positive region is within the edge of the AF (arrowheads). (**C-C″**) One section of the pectoral fin at 76 hpf (B) processed for three-color immunostaining [C, GFP (green) and Laminin α5 (magenta); C′, DAPI (gray); C″, merged image]. Scale bar: 50 μm. Arrow and arrowhead indicate the fin blood vessel and pAF/dAF boundary, respectively. (**D-H**) Lateral view of the pectoral fin buds. Scale bar: 100 μm. Arrow indicates the fin blood vessel. Arrowhead indicates the pAF/dAF boundary. (**I-J″**) High-magnification views of dAF cells (white brackets) at 46 (I-I″) and 70 (J-J″) hpf. Asterisk indicates not the AF but the endoskeletal region. Scale bars: 50 μm.

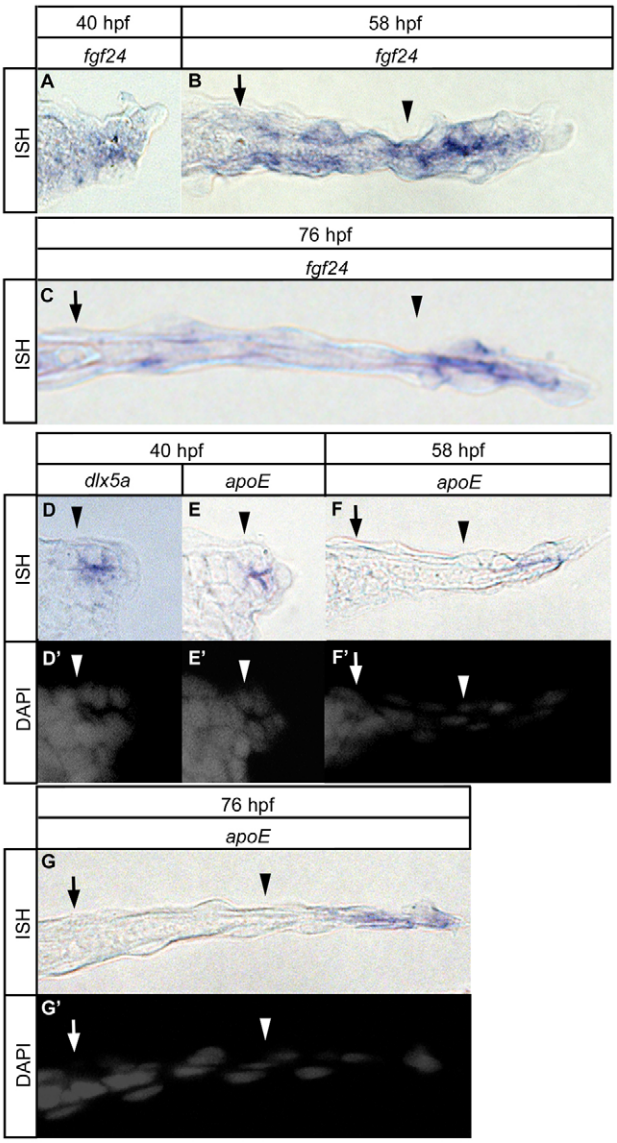

Fig. 4. Spatiotemporal expression pattern of AER/AF marker genes. (**A-G**) Spatial change of expression domain of *fgf24* (A-C), *dlx5a* (D) and *apoE* (E-G) at the indicated stages. D′-G′ show cell organization (gray: DAPI). Distal is to the right; dorsal is to the top in transverse sections. Arrows indicate circumferential fin blood vessel. Arrowheads indicate the base of the AF notch.

Gene expression in the AER/AF suggest different roles for the distal and proximal AF

The dAF-specific GFP expression pattern, implying a distinct function, led us to investigate dAF-specific expression of other genes. Although several genes have been shown to be expressed in the AER/AF (Monnot et al., 1999; Draper et al., 2003; Abe et al., 2007), detailed expression patterns at later pectoral fin bud stages have not been clarified. We found differential expression patterns of *fgf24* (*fibroblast growth factor 24*) (Draper et al., 2003), *dlx5a* (*distal-less homeobox gene 5a*) (Akimenko et al., 1994), *apoE* (*apolipoprotein E*) (Monnot et al., 1999) (Fig. 4) and *rspo2* (*predicted R-spondin 2*) (supplementary material Fig. S3) at later stages. In early AF formation (40 hpf), all of these genes were expressed throughout the AF epidermis (Fig. 4A,D,E), as reported above for the fin AER. However, at later stages, from 58 to 76 hpf, *fgf24* continued to be expressed in the entire AF epidermis (Fig. 4B,C), whereas transcripts of *apoE* (Fig. 4F,G) and *rspo2* (supplementary material Fig. S3) were distributed in the dAF. *dlx5a* expression disappeared by 58 hpf (not shown). These results support the idea that the AF region can be divided into two distinct regions (dAF and pAF) that have different tissue organization and gene functions.

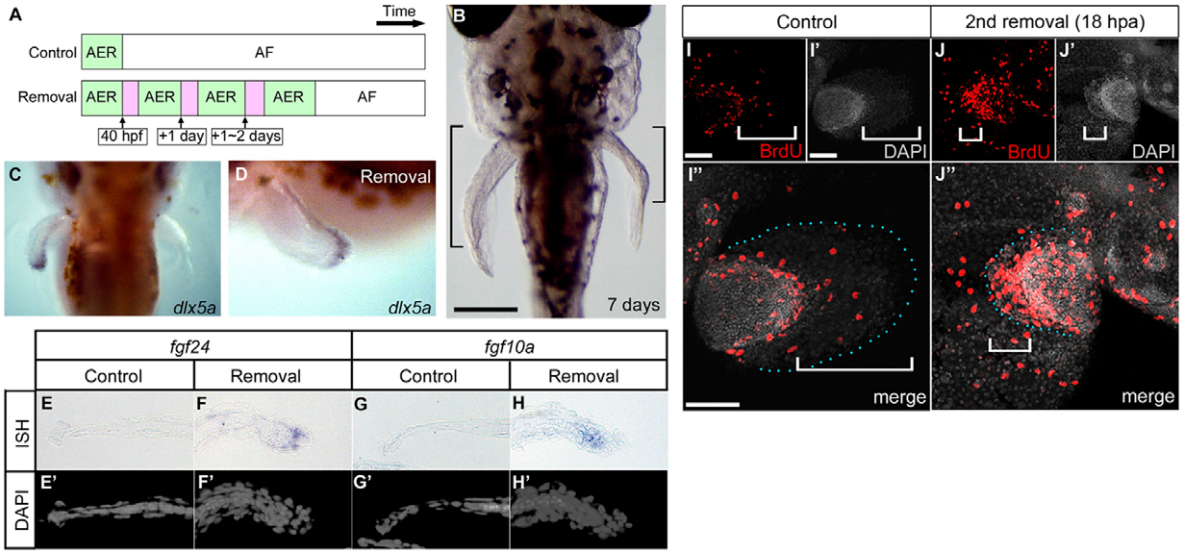

Fig. 5. Repeated AF removal caused prolonged developmental gene expression and excessive elongation of the endoskeletal region. (**A**) Experimental strategy for continuous AER presence. Bars indicate pectoral fin development time scale (control and removal sides of the fin). (**B**) A sample (7 days post-fertilization) after AF removal was performed three times on the left side of the pectoral fin bud. Black brackets indicate the endoskeletal region. Scale bar: 200 μm. (**C**,**D**) Dorsal and lateral views: 12 hours after the third AF removal, *dlx5a* was expressed in the re-formed AER (left side). (**E-H′**) Expression pattern of *fgf24* and *fgf10a* 12 hours after the third AF removal. *Fgf24* was expressed in the regenerating AER, and *fgf10a* was expressed in the distal portion of the endoskeletal region (F,H). Distal is to the left on the control side (E,E′,G,G′) and to the right on the AF removal side (F,F′,H,H′). (**I-J″**) Distribution of BrdU-positive cells after formation of a new AER. Whereas there are BrdU-positive cells at the distal edge of the endoskeletal region in the control side of the fin (I), in the side in which the AF had been removed, BrdU-positive cells are mainly located in the re-formed AER/AF region (white brackets) and in the endoskeletal region (J). Distal is to the right on the control side (I-I″) and to the left side on the AF removal side (J-J″). Blue dots indicate the fin margin. Scale bars: 100 μm in I,J.

AF function revealed by AF removal

Next, we investigated the role of AF at later stages of fin development. In both amniotes and teleosts, the AER is essential for the induction and outgrowth of the limb/fin buds (Grieshammer et al., 1996; Grandel et al., 2000; Kawakami et al., 2003; Mariani and Martin, 2003; Lu et al., 2008; Yu and Ornitz, 2008). The AF's function, by contrast, has not been described. Therefore, we decided to examine the effect of removing the AF microsurgically. In the AF ablation experiments at 40 hpf, when we could recognize the AF structure, only the ectoderm was removed, and the mesenchyme region for the endoskeleton, including the circumferential blood vessel, remained after the manipulation (supplementary material Fig. S4A-C). We observed no phenotype in the skeletal pattern of the endoskeletal elements (data not shown), unlike the deletion of distal elements observed after AER removal in amniote limb buds. Instead of distal truncation, we found that the endoskeletal region slightly extended distally (data not shown). Histological observations revealed that epidermis regenerated to reform a thickened AER structure within six hours of AF removal, and the AER was re-transformed into the AF by one day after AF removal (supplementary material Fig. S4D-F).

We thought that the slight extension of the endoskeletal region after AF removal might be due to extended exposure to the AER. Thus, we repeatedly removed the AF to expose the endoskeletal mesenchyme to the AER over a longer period, mimicking a delay of the transition from the AER to the AF (Fig. 5A; supplementary material Fig. S1E). Removing the AF three times resulted in excessive distal elongation of the endoskeletal region compared with the fin bud on the control side (n=13/15; Fig. 5B). In this process, the *dlx5a*, *fgf24* and *sp9* mRNAs were expressed in the regenerated AER and AF, and *fgf10a* and *mkp3* (*dusp6* – Zebrafish Information Network) were re-expressed in the endoskeletal mesenchyme region (Fig. 5C-H; data not shown). To examine cellular effects on fin buds by AF removal, we checked the distribution of BrdU-positive cells 18 hours after AF removal (done at 58 hpf; second removal time). Whereas there were BrdU-positive cells at the distal edge of the endoskeletal region in the control side of the fin (Fig. 5I), in the side in which the AF had been removed, BrdU-positive cells were located broadly (with large numbers both in the re-formed AER/AF region and in the endoskeletal region) (n=13/16; Fig. 5J). It is possible that the re-induced AER signals kept the mesenchyme in an undifferentiated and growth state, even though the control side of the fin bud had already started differentiating.

After two weeks, as a result of repeatedly (three times) removing the AF, the endoskeletal disc was deformed and appeared more oblong along the PD axis than that of the control fin (Fig. 6A,B). PD length of the disc was increased (Fig. 6C; supplementary material Table S2), but the change in width along the anteroposterior axis was not significant (Fig. 6D; supplementary material Table S2). After two months, the morphology of the resultant endochondral bones, the proximal and distal radials, was affected in adult fins (n=6/6; Fig. 6E-H, see also supplementary material Fig. S5). In normal pectoral fins, an endoskeletal disc is subdivided into four parts and differentiates into four proximal radials, while six to eight distal radials are dotted distal to the proximal radials (Fig. 6E,G) (Grandel and Schulte-Merker, 1998). After removing the AF three times, a sample (Fig. 6F,H) had only three proximal radials, and the fourth radial was missing or fused with the third one. In this sample, the second and third radials had widened and adhered to each other, and the third radial appeared to be divided into two along the PD axis. An additional distal radial

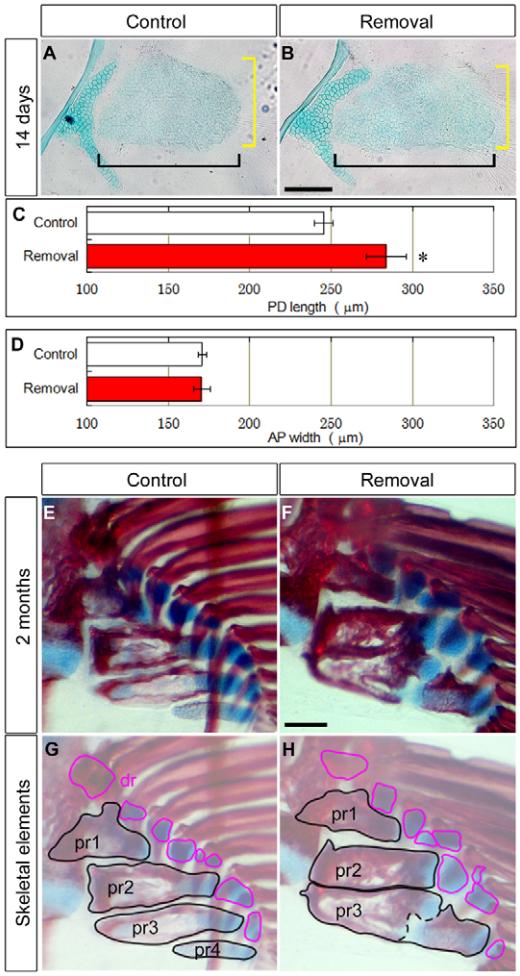

Fig. 6. Repeated AF removal affected endoskeletal bones. (**A**,**B**) Alcian Blue staining of the pectoral fin 14 days after AF removal (three times). Scale bar: 100 μm. (**C**,**D**) PD length (C, black brackets in A,B) and AP width (D, yellow brackets in A,B) of endoskeletal disc after removing the AF three times. Error bars indicate s.e.m. Data were analyzed by Student's *t*-test (*P<0.05). Measurements are shown in supplementary material Table S2. (**E-H**) Alcian Blue and Alizarin Red staining of the pectoral fin 2 months after AF removal. Specimens (E,F) are outlined and highlighted, focusing on endoskeletal bones (G,H). Proximal radials (pr) are outlined in black. Distal radials (dr) are outlined in red. Scale bar: 100 μm.

had formed between the proximal and distal radials (supplementary material Fig. S5A). Thus, removal of the AF three times caused excessive distal fin bud outgrowth and gave rise to changes in endoskeletal morphology, suggesting that the temporal range of exposure to AER signals controls the outgrowth and morphology of the endoskeletal region. The AER-to-AF transition might restrict the growth and shape of the endoskeletal region.

Effect of distal AF removal on pAF region growth

Although entirely removing the early AF suggested that the AER-AF transition has roles in endoskeletal patterning, it could not reveal the function of the AF itself. To examine the role of the AF, we removed only the dAF at a later stage, 53 hpf, when it could be visualized by a GFP reporter (Fig. 7). When the whole dAF was removed, the pAF stopped growing for ~24 hours (Fig. 7A-C), but resumed outgrowth after the dAF formed again. The length of the manipulated AF caught up with that of the control by 36 hours (Fig. 7D). These results suggest that the dAF has a crucial function in AF elongation. To clarify dAF's function further, we next removed either half of the dAF to examine the effect directly in the same fin. When the anterior half of the dAF was removed (Fig. 7E,F), the remaining anterior half of the pAF stopped growing for ~24 hours and a shortened AF was seen at the removal site (Fig. 7G). After 36 hours, the length of the AF at the removal site had recovered (Fig. 7H). Removing the dAF posterior half caused delay in posterior pAF outgrowth (n=3/4, not shown). It is likely that dAF signals play roles in the elongation and outgrowth of the pAF region. In contrast to the AF removal in early stages, the endoskeletal region was not affected by dAF removal, suggesting that dAF signals play roles restricted to the AF region.

As a candidate of the epidermal signal, we examined FGF function in elongation of the AF by a pharmacological assay with a specific blocker of Fgf signaling, SU5402 (supplementary material Fig. S6, Table S3). After SU5402 treatment, the AF elongation was significantly diminished. However, the endoskeletal region was also affected, and it is possible that the AF reduction by SU5402 might be due to a secondary effect of a disorder in the fin mesenchyme. These results suggest that the Fgf signaling pathway is important for fin outgrowth but that its function is not specific to the AF region.

Ectodermal cell shape controls AF outgrowth

The results described above showed that AF outgrowth is caused under the control of dAF signals. Interestingly, immunostaining for BrdU (supplementary material Fig. S7) and active Caspase 3 (data not shown) did not show any significant deviation in cell proliferation or death in the developing fin bud epidermal layer, suggesting that other changes, such as changes in the AF epidermal cell shape (shape of nuclei in Fig. 1C-G, and cell shape in Fig. 3I,J) and in extracellular matrix accumulation, led to extension of the dAF/pAF region.

To confirm the importance of changes in ectodermal cell shape, we observed two types of pectoral fin phenotype in HG21C embryos (*tcf7* mutant fish) and LiCl-treated embryos. Nagayoshi et al. previously reported that disruption of the *tcf7* gene, which encodes a transcription factor mediating Wnt signaling, resulted in mildly shortened and wavy AF and MFF (Nagayoshi et al., 2008), but no further details about fin phenotypes are known. In order to understand the fin shrinkage, we observed ectodermal cell shape in the pectoral fin of *tcf7* mutants and measured the lengths of the endoskeletal region and the AF region at 70 hpf (Fig. 8). The pectoral fin bud of the homozygous mutants was dwarfish (Fig. 8D,D′) compared with the control fin (heterozygous mutant; Fig. 8B,B′). We found that the AF ectodermal cell shape was disorganized in homozygous mutants of *tcf7* (Fig. 8C′,D′) compared with the hexagonal cell shape of the control AF (Fig. 8A′,B′). We also found that AF formation was incomplete, although the endoskeletal region developed normally (Fig. 8E). We did not observe disorders of initiation of the pectoral fin bud in *tcf7* homozygous mutants before AF formation (supplementary material Fig. S8) as reported previously (Nagayoshi et al., 2008), suggesting that the HG21C fish gives rise to a short fin phenotype not by inherent entire fin defects but by disruption of the AF ectodermal cell organization.

Furthermore, when well-developed pectoral fins (70 hpf) were treated with 0.3 M LiCl, the AF shrank along the PD axis (supplementary material Fig. S9A). Interestingly, as the fin buds

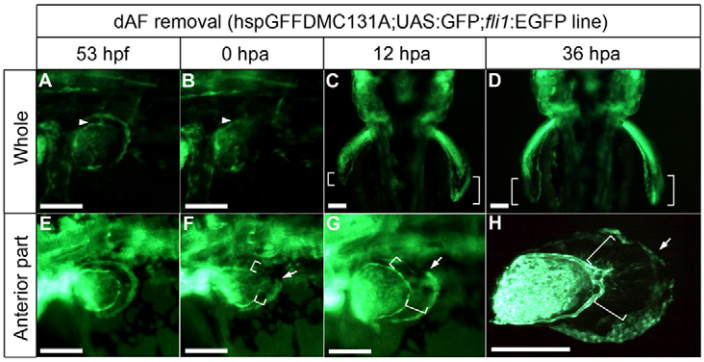

Fig. 7. Distal AF removal affected AF outgrowth. The dAF is visualized in the hspGFFDMC131A;UAS:GFP line; the AF base is shown by *fli1*:EGFP (arrowheads). (**A-C**) When the dAF was completely removed from the left fin (B), pAF (GFP-negative) development was delayed compared with the control side (C) (*n*=3/3; white brackets). (**D**) By 36 hours post-amputation (hpa), the AF length (white brackets) had returned to normal. (**E-G**) When the anterior part of the dAF was removed (E,F), only the anterior pAF development was delayed (*n*=6/8; compare with white brackets in E,F). (**H**) By 36 hpa, the fin shape had returned to normal. Arrows represent the removed/unremoved boundary. The pectoral fin bud was dissected from the fish body and mounted on a glass slide. Scale bars: 200 μm in A,B,E-H; 20 μm in C,D.

were not completely lost and the proximal part was not affected, there was no resultant change in the endoskeletal region's size or shape. We found that epithelial cells had a polygonal shape in the normal AF (Fig. 8F-G′), but after LiCl treatment, cell shape had collapsed in four or five rows of ectodermal cells within the whole AF along the PD axis (Fig. 8H-I′). The morphology of the MFF cells was also affected by LiCl treatment (supplementary material Fig. S9B-D).

These observations suggest that changes in AF cell shape along the PD axis play a crucial role in AF outgrowth and increase in its size at later stages of fin development.

DISCUSSION

AF morphogenesis

We showed that AER elongation began at ~36 hpf and that the structure grew considerably in the distal direction. We define the elongated epidermal structure after 36 hpf as the AF, which has a double-layered basement membrane between the epidermal sheets. Consistent with these histological aspects, *fgf4* and *fgf8*, which are AER markers in the amniote limb, are expressed in the AF after 36 hpf, whereas *fgf16* and *fgf24* are preferentially expressed in the AER before 34 hpf (Fischer et al., 2003; Nomura et al., 2006). These findings indicate that the AER-AF transition phenomenon is accompanied by histological and molecular changes at ~36 hpf in the pectoral fin bud. The basement membrane is recognizable by an accumulation of Laminin α5, which plays a role in establishing the AF (Dane and Tucker, 1985; Webb et al., 2007), and the elongating AF can then be divided into two parts: the dAF and the pAF. The pAF is the proximal portion, into which the mesenchymal cells migrate. The proximal end of the pAF borders on the endoskeletal region, and the circumferential blood vessel surrounding the endoskeletal region divides the fin bud into the fin ray region and the endoskeletal region. As precise cell lineage tracing of the fin ectoderm has not been successful, it is not clear where AF cells come from. It is both possible that non-AER ectodermal cells participate in the development of dAF and pAF and that AER cells form them. Considering the reduced proliferation of ectodermal cells (supplementary material Fig. S7), we speculate that some non-AER cells convert to AF cells; recruitment of adjacent epithelial cells might contribute to fold elongation.

Conservation of and differences between fin and limb epidermal structures in development

The dAF, which retains a double-layered, back-to-back basement membrane with no mesenchyme therein, appears to have a distinct function. This distinct epithelial region is recognizable by GFP-positive epidermal cells in hspGFFDMC131A;UAS:GFP fish. The hspGFFDMC131A insertion was close to the *rspo2* gene and presumably trapped its enhancer activity. Interestingly, *rspo2* is crucial for AER maintenance, and *rspo2* knockout mice have limb defects (lack of fibula or distal phalangeal bones) (Nam et al., 2007; Aoki et al., 2008), but the functions of the *rspo2* gene in fin development remain unknown. Regarding another dAF signal, Gautier et al. (Gautier et al., 2008) showed that some members of *fras1*/*frem* gene family are expressed in the distal margin of the pectoral fin bud. We examined the expression of these genes and found that *frem2a* expression was stronger in the dAF than in the pAF (Yano and Tamura, 2012). Interestingly, we also found GFP-positive cells in the pectoral fin AER prior to the transition in hspGFFDMC131A;UAS:GFP fish, suggesting a common function in the AER and dAF. This is also supported by the finding that some genes, including *apoE*, were expressed in both the AER and the dAF. The expression of *apoE* has been shown in the distal margin of the bud (Monnot et al., 1999); the *apoE*-positive region at later stages should be the dAF. GFP was also found in the distal margin of the MFF in the double-transgenic fish. Thus, there might be shared mechanisms in AF and MFF formation and function. Further studies are needed to understand the similarities in fin AER/AF (pAF and dAF) and MFF function, and the evolutional conservation of that function among these structures and the limb AER. Although the nature of the epidermal signals remains unknown, our results obtained by using an FGF-signaling inhibitor suggest that the signaling pathway is a good candidate. Nevertheless, the function of FGF signaling in the AF remains inconclusive because the inhibitor treatment did not cause complete loss of the AF, and contribution of other signals is probable.

Many studies, including investigations of the fin AER's function in development of the endoskeletal region (Grandel et al., 2000; Norton et al., 2005), have suggested that the limb and fin AERs correspond to each other functionally, and thus previous studies have focused on conservation and similarity of mechanisms between the limb AER and fin AER. Little was known about the diversity and differences between them despite their clear developmental and morphological differences. Removal of the dAF delayed pAF outgrowth, suggesting that the dAF plays a role in pAF outgrowth. AER signals before the transition are necessary for the survival, growth and maintenance of an undifferentiated state of 'mesenchyme', and the dAF at the apex of the expanding AF might have the same function against the AF 'epidermis'. The region responding to the epidermal signals should change from the endoskeletal region to the AF region at the time of the AER-to-AF transition (Fig. 9).

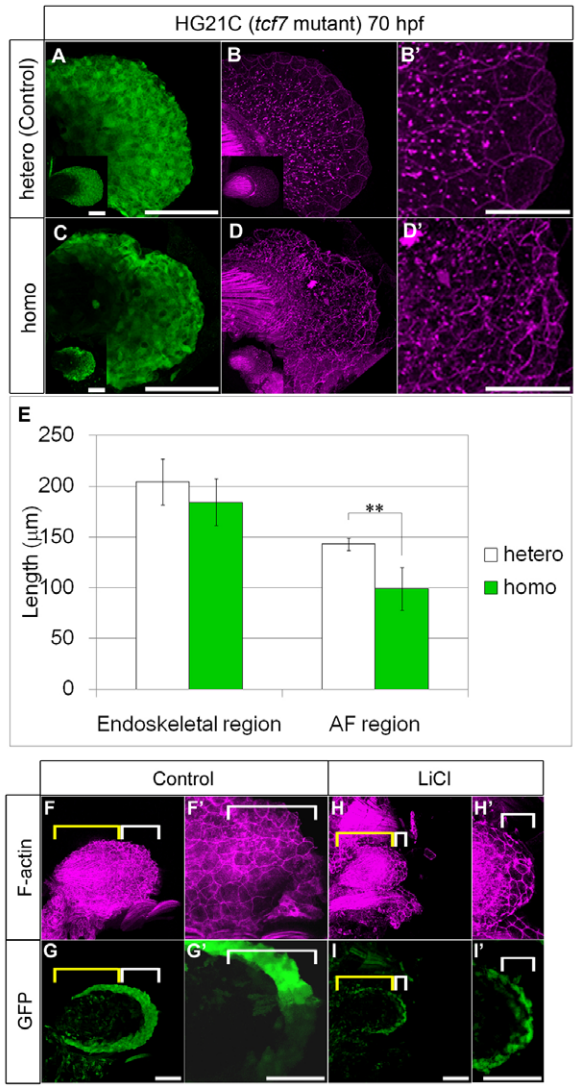

Fig. 8. Disruption of cell shape caused AF shrinkage. (**A-E**) Heterozygotes for control (A,B) and homozygotes (C,D) of *tcf7* mutants [HG21C line (Nagayoshi et al., 2008)]. The AF is shortened and wavy with abnormal shrunken cells (C,D). Insets (bottom left in A-D) show images of whole fin and high magnification of the cell shape is shown in B′,D′. (E) PD lengths of the endoskeletal region (left) and AF region (right) at 70 hpf in heterozygotes (n=12) and homozygotes (n=9). Measurements are shown in supplementary material Table S4. Data were analyzed by Student's t-test (**P<0.001). Error bars indicate s.d. (**F-I′**) LiCl treatment. Cytoskeletal disruption of the AF was detected by immunostaining for F-actin (magenta) using the hspGFFDMC131A;UAS:GFP fish (green). About five rows of ectodermal cells (white brackets) were located in the control fin (0.3 M NaCl) (F,G, high magnification of the AF in F′,G′). The LiCl-treated fin had the same number of ectodermal rows as the control, but the cells were flattened along the PD axis (H,I, magnification of the AF in H′,I′). Note that the endoskeletal region (yellow brackets) was hardly affected in this experiment. Scale bars: 100 μm in A,C,F-I′; 50 μm in B′,D′.

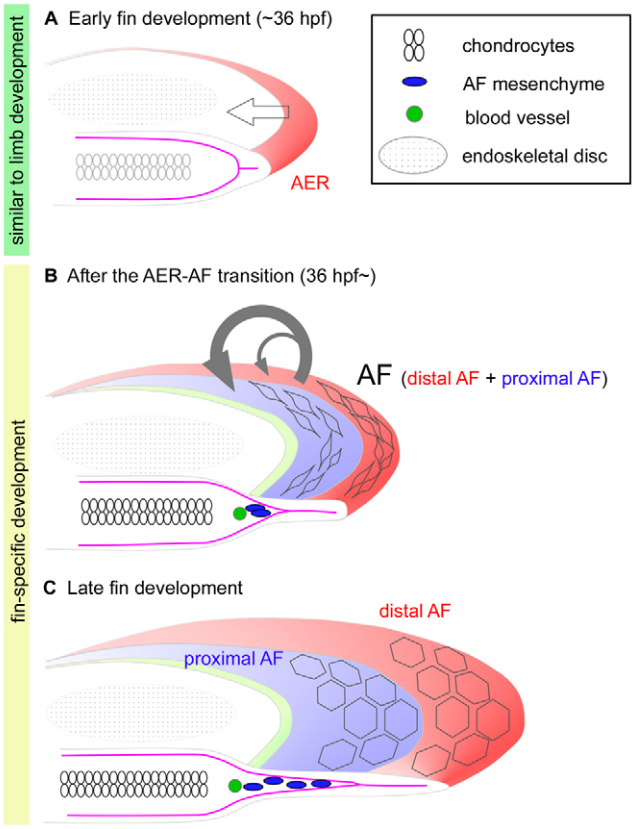

Fig. 9. A model of pectoral fin development. (**A**) Until 36 hpf, the AER (red) is crucial for fin mesenchyme outgrowth (straight arrow). (**B**) After AER-AF transition, the dAF acts on the outgrowth of the AF (curved arrows). (**C**) Later, the dAF is distinguished from the pAF by tissue organization and gene expression. As fin buds develop distally, the ectodermal cell shape in the AF changes from a spherical and slender morphology (B) to a thin, polygonal one (C).

Cell-shape changes mediate the mechanism of apical fold outgrowth

Although ectodermal cells proliferate markedly in the amniote AER (Fernandez-Teran et al., 2006), there was no significant proliferation in the teleost fin AER or AF (supplementary material Fig. S7), suggesting that cell proliferation cannot directly explain AF outgrowth. Apoptosis also occurs in the AER in the limb bud (Fernandez-Teran et al., 2006). If cell death also occurs in the AER in the early fin bud, and the AF stops dying after AER-to-AF transition, the number of ectodermal cells might increase. However, observations of cell death (Camarata et al., 2010) (our unpublished observation), showing few dying cells both in the fin AER and AF, ruled out this possibility. We confirmed that ectodermal cells in the AF have a spindle shape at early stages and then become flattened, as suggested by Dane and Tucker (Dane and Tucker, 1985). Here, we propose that a change to a flattened or enlarged ectodermal cell shape is important for AF outgrowth (Fig. 9). After the AER-AF transition, the AF starts to develop distally with little proliferation, and the shape of AF cells changes. We demonstrated a unique phenotype of AF outgrowth by disruption of Tcf7-related pathways. These are new insights into fin development, but further investigation is needed to identify candidate signaling cascades for ectodermal cell organization. It is noteworthy that AF formation still occurs in the *tcf7* mutant but that double knockdown of *tcf7* and *lef1*, both of which are targets of the Wnt canonical pathway, causes complete loss of pectoral fins (Nagayoshi et al., 2008). Tcf7 is also involved in Notch signaling (D'Angelo et al., 2010; Germar et al., 2011). Moreover, LiCl treatment affects several pathways (e.g. Wnt canonical pathway, Wnt/JNK pathway, actin cytoskeleton

and microtubule dynamics) (Cohen and Frame, 2001; Grimes and Jope, 2001; Eldar-Finkelman, 2002; Kaytor and Orr, 2002; Pandur et al., 2002; Doble and Woodgett, 2003; Kawano and Kypta, 2003; Sun et al., 2009), and results of further studies should provide an insight into the molecular mechanisms of AF morphogenesis. Signals from the dAF are crucial for AF outgrowth (Fig. 7) and may act as both autocrine signals in the dAF and paracrine signals to the pAF to flatten the ectodermal cell shape. Mesenchyme that has migrated into the pAF and actinotrichia as a supporting material might play a supportive role in AF extension because lack of them gives rise to an abnormal and reduced shape of the AF, although in the absence of them, the AF or MFF can be elongated at the early stage of AF/MFF development (Sakaguchi et al., 2006; Zhang et al., 2010).

The clock model and appendage evolution

Repeated AF removal elongated rather than truncated the endoskeletal region along the PD axis, which is striking because AER removal in the tetrapod limb bud is known to result in distal truncation and never in elongation. Interestingly, cellular proliferation status is changed by AF removal. Mesenchymal cell proliferation increases beneath a newly formed AER. Prolonged AER formation seems to cause distal outgrowth of the endoskeleton and to give rise to extra elements in the resultant skeleton. By contrast, AP width of the endoskeletal region was not changed, but the final skeletal patterns tended to be reduced along the AP axis (skeletal fusion of proximal radials). The cause of AP deformation remains vague, and some morphogenetic conditions in the endoskeletal region might be changed at a much later stage, following or accompanying morphological change along the PD axis. Our analyses of gene expression suggest that the PD elongates owing to repeated AER signal exposure, which is thought to prolong many signal pathways for morphogenesis in the endoskeletal region. The pathways might include the Shh pathway, which is known to have a feedback loop with the AER, because activating the signaling pathway elongates the endoskeletal disc (Sakamoto et al., 2009). We cannot eliminate the possibility of side effects of AF surgery, because of technical limitation of experimental embryology; other methods, such as non-surgical induction or inhibition of the AER-AF transition, will help to further clarify the AER/AF function. The AER and AF also appear to have different functions in the endoskeletal region. The dAF is distanced from the endoskeletal region as fin development proceeds, and cannot continue to regulate the morphogenesis of the endoskeletal region (Fig. 9). Thus, the AER-to-AF transition marks a time at which the AER/AF responding region shifts from the endoskeletal region to the AF.

This interpretation reminds us of the clock model (supplementary material Fig. S1), which explains fin-to-limb transition in evolution as a heterochronic shift of the timing of AER-to-AF transition (Thorogood, 1991; Sordino et al., 1995; Freitas et al., 2007; Yano and Tamura, 2012). Our data from prolonged experimental AER signal exposure in the fin bud support the clock model. It is possible that repeatedly removing the AF prolonged the period of exposure to AER signals, altering the gene expression, endochondral disc shape, and endoskeletal pattern. It is noteworthy that implanting an FGF bead at a certain stage of chick limb development causes the unusual elongation of a digit (Uejima et al., 2010), and extended maintenance of the AER in the dolphin limb bud correlates with hyperphalangy in the digits (Richardson and Oelschlager, 2002).

Our findings suggest that early AF formation causes less endoskeleton patterning along the PD axis than does late AF formation. Therefore, extremely late AF formation, that is, AF loss, might have enabled early tetrapods to acquire a well-elongated and segmented pattern of limb skeleton. Throughout the present article, we have shown both similarities (in the formation and function of the AER) and differences (in the formation and function of the AF) between the developmental programs for fins and limbs. We propose that these developmental data help explain the deep homology in genetic networks and the variety of limb and fin structures (Shubin et al., 2009). Further investigations of teleost fin development at the cellular and molecular levels will elucidate further the fin-to-limb transition from an evolutionary development perspective.

Acknowledgements

We thank Dr Sumio Isogai for providing the *fli1*:EGFP y1 transgenic strain; Dr Seiji Nakano for advice for confocal imaging; and Dr Makoto Suzuki for advice for sample sectioning and mounting. We are grateful to Dr Akiha Nishihara-Kawasaki, Dr Yuji Takemoto and Hiroki Yoshihara for excellent fish care. Three anonymous reviewers provided constructive comments that substantially improved this paper.

Funding

This work was supported by research grants from KAKENHI (Grant-in-Aid for Scientific Research) [21370095] and from the Funding Program for Next Generation World-Leading Researchers [LS007] from the Cabinet Office, Government of Japan. T.Y. was supported by Japan Society for the Promotion of Science (JSPS) Research Fellowships for Young Scientists, Japan.

Competing interests statement

The authors declare no competing financial interests.

Supplementary material

Supplementary material available online at
http://dev.biologists.org/lookup/suppl/doi:10.1242/dev.075572/-/DC1

References

Abe, G., Ide, H. and Tamura, K. (2007). Function of FGF signaling in the developmental process of the median fin fold in zebrafish. *Dev. Biol.* **304**, 355-366.

Ahn, D. and Ho, R. K. (2008). Tri-phasic expression of posterior Hox genes during development of pectoral fins in zebrafish: implications for the evolution of vertebrate paired appendages. *Dev. Biol.* **322**, 220-233.

Akimenko, M. A., Ekker, M., Wegner, J., Lin, W. and Westerfield, M. (1994). Combinatorial expression of three zebrafish genes related to distal-less: part of a homeobox gene code for the head. *J. Neurosci.* **14**, 3475-3486.

Aoki, M., Kiyonari, H., Nakamura, H. and Okamoto, H. (2008). R-spondin2 expression in the apical ectodermal ridge is essential for outgrowth and patterning in mouse limb development. *Dev. Growth Differ.* **50**, 85-95.

Asakawa, K., Suster, M. L., Mizusawa, K., Nagayoshi, S., Kotani, T., Urasaki, A., Kishimoto, Y., Hibi, M. and Kawakami, K. (2008). Genetic dissection of neural circuits by Tol2 transposon-mediated Gal4 gene and enhancer trapping in zebrafish. *Proc. Natl. Acad. Sci. USA* **105**, 1255-1260.

Boisvert, C. A., Mark-Kurik, E. and Ahlberg, P. E. (2008). The pectoral fin of Panderichthys and the origin of digits. *Nature* **456**, 636-638.

Camarata, T., Snyder, D., Schwend, T., Klosowiak, J., Holtrup, B. and Simon, H. G. (2010). Pdlim7 is required for maintenance of the mesenchymal/epidermal Fgf signaling feedback loop during zebrafish pectoral fin development. *BMC Dev. Biol.* **10**, 104.

Cohen, P. and Frame, S. (2001). The renaissance of GSK3. *Nat. Rev. Mol. Cell Biol.* **2**, 769-776.

Dane, P. J. and Tucker, J. B. (1985). Modulation of epidermal cell shaping and extracellular matrix during caudal fin morphogenesis in the zebra fish *Brachydanio rerio*. *J. Embryol. Exp. Morphol.* **87**, 145-161.

D'Angelo, A., Bluteau, O., Garcia-Gonzalez, M. A., Gresh, L., Doyen, A., Garbay, S., Robine, S. and Pontoglio, M. (2010). Hepatocyte nuclear factor 1alpha and beta control terminal differentiation and cell fate commitment in the gut epithelium. *Development* **137**, 1573-1582.

Doble, B. W. and Woodgett, J. R. (2003). GSK-3: tricks of the trade for a multi-tasking kinase. *J. Cell Sci.* **116**, 1175-1186.

Draper, B. W., Stock, D. W. and Kimmel, C. B. (2003). Zebrafish fgf24 functions with fgf8 to promote posterior mesodermal development. *Development* **130**, 4639-4654.

Eldar-Finkelman, H. (2002). Glycogen synthase kinase 3, an emerging therapeutic target. *Trends Mol. Med.* **8**, 126-132.
Fagotto, F. and Gumbiner, B. M. (1994). Beta-Catenin localization during *Xenopus* embryogenesis – accumulation at tissue and somite boundaries. *Development* **120**, 3667-3679.
Fernandez-Teran, M. A., Hinchliffe, J. R. and Ros, M. A. (2006). Birth and death of cells in limb development: a mapping study. *Dev. Dyn.* **235**, 2521-2537.
Fischer, S., Draper, B. W. and Neumann, C. J. (2003). The zebrafish fgf24 mutant identifies an additional level of Fgf signaling involved in vertebrate forelimb initiation. *Development* **130**, 3515-3524.
Freitas, R., Zhang, G. and Cohn, M. J. (2007). Biphasic Hoxd gene expression in shark paired fins reveals an ancient origin of the distal limb domain. *PLoS ONE* **2**, e754.
Gautier, P., Naranjo-Golborne, C., Taylor, M. S., Jackson, I. J. and Smyth, I. (2008). Expression of the fras1/frem gene family during zebrafish development and fin morphogenesis. *Dev. Dyn.* **237**, 3295-3304.
Germar, K., Dose, M., Konstantinou, T., Zhang, J., Wang, H., Lobry, C., Arnett, K. L., Blacklow, S. C., Aifantis, I., Aster, J. C. et al. (2011). T-cell factor 1 is a gatekeeper for T-cell specification in response to Notch signaling. *Proc. Natl. Acad. Sci. USA* **108**, 20060-20065.
Grandel, H. and Schulte-Merker, S. (1998). The development of the paired fins in the zebrafish (*Danio rerio*). *Mech. Dev.* **79**, 99-120.
Grandel, H., Draper, B. W. and Schulte-Merker, S. (2000). dackel acts in the ectoderm of the zebrafish pectoral fin bud to maintain AER signaling. *Development* **127**, 4169-4178.
Grieshammer, U., Minowada, G., Pisenti, J. M., Abbott, U. K. and Martin, G. R. (1996). The chick limbless mutation causes abnormalities in limb bud dorsal-ventral patterning: implications for the mechanism of apical ridge formation. *Development* **122**, 3851-3861.
Grimes, C. A. and Jope, R. S. (2001). The multifaceted roles of glycogen synthase kinase 3beta in cellular signaling. *Prog. Neurobiol.* **65**, 391-426.
Hall, B. K. (2005). *Bones And Cartilage: Developmental And Evolutionary Skeletal Biology*. London: Elsevier Academic Press.
Isogai, S., Horiguchi, M. and Weinstein, B. M. (2001). The vascular anatomy of the developing zebrafish: an atlas of embryonic and early larval development. *Dev. Biol.* **230**, 278-301.
Joly, J. S., Joly, C., Schulte-Merker, S., Boulekbache, H. and Condamine, H. (1993). The ventral and posterior expression of the zebrafish homeobox gene eve1 is perturbed in dorsalized and mutant embryos. *Development* **119**, 1261-1275.
Kawakami, Y., Rodriguez-Leon, J., Koth, C. M., Buscher, D., Itoh, T., Raya, A., Ng, J. K., Esteban, C. R., Takahashi, S., Henrique, D. et al. (2003). MKP3 mediates the cellular response to FGF8 signalling in the vertebrate limb. *Nat. Cell Biol.* **5**, 513-519.
Kawakami, Y., Esteban, C. R., Matsui, T., Rodriguez-Leon, J., Kato, S. and Izpisua Belmonte, J. C. (2004). Sp8 and Sp9, two closely related buttonhead-like transcription factors, regulate Fgf8 expression and limb outgrowth in vertebrate embryos. *Development* **131**, 4763-4774.
Kawano, Y. and Kypta, R. (2003). Secreted antagonists of the Wnt signalling pathway. *J. Cell Sci.* **116**, 2627-2634.
Kaytor, M. D. and Orr, H. T. (2002). The GSK3 beta signaling cascade and neurodegenerative disease. *Curr. Opin. Neurobiol.* **12**, 275-278.
Kimmel, C. B., Ballard, W. W., Kimmel, S. R., Ullmann, B. and Schilling, T. F. (1995). Stages of embryonic development of the zebrafish. *Dev. Dyn.* **203**, 253-310.
Lawson, N. D. and Weinstein, B. M. (2002). In vivo imaging of embryonic vascular development using transgenic zebrafish. *Dev. Biol.* **248**, 307-318.
Long, J. A., Young, G. C., Holland, T., Senden, T. J. and Fitzgerald, E. M. (2006). An exceptional Devonian fish from Australia sheds light on tetrapod origins. *Nature* **444**, 199-202.
Lu, P., Yu, Y., Perdue, Y. and Werb, Z. (2008). The apical ectodermal ridge is a timer for generating distal limb progenitors. *Development* **135**, 1395-1405.
Mariani, F. V. and Martin, G. R. (2003). Deciphering skeletal patterning: clues from the limb. *Nature* **423**, 319-325.
Mercader, N. (2007). Early steps of paired fin development in zebrafish compared with tetrapod limb development. *Dev. Growth Differ.* **49**, 421-437.
Metscher, B. D., Takahashi, K., Crow, K., Amemiya, C., Nonaka, D. F. and Wagner, G. P. (2005). Expression of Hoxa-11 and Hoxa-13 in the pectoral fin of a basal ray-finned fish, *Polyodon spathula*: implications for the origin of tetrapod limbs. *Evol. Dev.* **7**, 186-195.
Monnot, M. J., Babin, P. J., Poleo, G., Andre, M., Laforest, L., Ballagny, C. and Akimenko, M. A. (1999). Epidermal expression of apolipoprotein E gene during fin and scale development and fin regeneration in zebrafish. *Dev. Dyn.* **214**, 207-215.
Nagayoshi, S., Hayashi, E., Abe, G., Osato, N., Asakawa, K., Urasaki, A., Horikawa, K., Ikeo, K., Takeda, H. and Kawakami, K. (2008). Insertional mutagenesis by the Tol2 transposon-mediated enhancer trap approach generated mutations in two developmental genes: tcf7 and synembryn-like. *Development* **135**, 159-169.
Nam, J. S., Park, E., Turcotte, T. J., Palencia, S., Zhan, X., Lee, J., Yun, K., Funk, W. D. and Yoon, J. K. (2007). Mouse R-spondin2 is required for apical ectodermal ridge maintenance in the hindlimb. *Dev. Biol.* **311**, 124-135.
Nechiporuk, A. and Keating, M. T. (2002). A proliferation gradient between proximal and msxb-expressing distal blastema directs zebrafish fin regeneration. *Development* **129**, 2607-2617.
Nomura, R., Kamei, E., Hotta, Y., Konishi, M., Miyake, A. and Itoh, N. (2006). Fgf16 is essential for pectoral fin bud formation in zebrafish. *Biochem. Biophys. Res. Commun.* **347**, 340-346.
Norton, W. H., Ledin, J., Grandel, H. and Neumann, C. J. (2005). HSPG synthesis by zebrafish Ext2 and Extl3 is required for Fgf10 signalling during limb development. *Development* **132**, 4963-4973.
Pandur, P., Lasche, M., Eisenberg, L. M. and Kuhl, M. (2002). Wnt-11 activation of a non-canonical Wnt signalling pathway is required for cardiogenesis. *Nature* **418**, 636-641.
Richardson, M. K. and Oelschlager, H. H. (2002). Time, pattern, and heterochrony: a study of hyperphalangy in the dolphin embryo flipper. *Evol. Dev.* **4**, 435-444.
Sakaguchi, S., Nakatani, Y., Takamatsu, N., Hori, H., Kawakami, A., Inohaya, K. and Kudo, A. (2006). Medaka unextended-fin mutants suggest a role for Hoxb8a in cell migration and osteoblast differentiation during appendage formation. *Dev. Biol.* **293**, 426-438.
Sakamoto, K., Onimaru, K., Munakata, K., Suda, N., Tamura, M., Ochi, H. and Tanaka, M. (2009). Heterochronic shift in Hox-mediated activation of sonic hedgehog leads to morphological changes during fin development. *PLoS ONE* **4**, e5121.
Shubin, N. H., Daeschler, E. B. and Jenkins, F. A., Jr (2006). The pectoral fin of *Tiktaalik roseae* and the origin of the tetrapod limb. *Nature* **440**, 764-771.
Shubin, N., Tabin, C. and Carroll, S. (2009). Deep homology and the origins of evolutionary novelty. *Nature* **457**, 818-823.
Sordino, P., van der Hoeven, F. and Duboule, D. (1995). Hox gene expression in teleost fins and the origin of vertebrate digits. *Nature* **375**, 678-681.
Sun, T., Rodriguez, M. and Kim, L. (2009). Glycogen synthase kinase 3 in the world of cell migration. *Dev. Growth Differ.* **51**, 735-742.
Suzuki, M., Hara, Y., Takagi, C., Yamamoto, T. S. and Ueno, N. (2010). MID1 and MID2 are required for *Xenopus* neural tube closure through the regulation of microtubule organization. *Development* **137**, 2329-2339.
Tamura, K., Yonei-Tamura, S., Yano, T., Yokoyama, H. and Ide, H. (2008). The autopod: its formation during limb development. *Dev. Growth Differ.* **50 Suppl. 1**, S177-S187.
Thorogood, P. (1991). The development of the teleost fin and implications for our understanding of tetrapod evolution. In *Developmental Patterning Of The Vertebrate Limb* (ed. J. Hinchliffe, J. Hurle and D. Summerbell), pp. 347-354. London: Plenum Press.
Todt, W. L. and Fallon, J. F. (1984). Development of the apical ectodermal ridge in the chick wing bud. *J. Embryol. Exp. Morphol.* **80**, 21-41.
Uejima, A., Amano, T., Nomura, N., Noro, M., Yasue, T., Shiroishi, T., Ohta, K., Yokoyama, H. and Tamura, K. (2010). Anterior shift in gene expression precedes anteriormost digit formation in amniote limbs. *Dev. Growth Differ.* **52**, 223-234.
Webb, A. E., Sanderford, J., Frank, D., Talbot, W. S., Driever, W. and Kimelman, D. (2007). Laminin alpha5 is essential for the formation of the zebrafish fins. *Dev. Biol.* **311**, 369-382.
Woltering, J. M. and Duboule, D. (2010). The origin of digits: expression patterns versus regulatory mechanisms. *Dev. Cell* **18**, 526-532.
Wood, A. and Thorogood, P. (1984). An analysis of in vivo cell migration during teleost fin morphogenesis. *J. Cell Sci.* **66**, 205-222.
Yano, T. and Tamura, K. (2012). The making of differences between fins and limbs. *J. Anat.* (in press).
Yonei-Tamura, S., Abe, G., Tanaka, Y., Anno, H., Noro, M., Ide, H., Aono, H., Kuraishi, R., Osumi, N., Kuratani, S. et al. (2008). Competent stripes for diverse positions of limbs/fins in gnathostome embryos. *Evol. Dev.* **10**, 737-745.
Yu, K. and Ornitz, D. M. (2008). FGF signaling regulates mesenchymal differentiation and skeletal patterning along the limb bud proximodistal axis. *Development* **135**, 483-491.
Zhang, J., Wagh, P., Guay, D., Sanchez-Pulido, L., Padhi, B. K., Korzh, V., Andrade-Navarro, M. A. and Akimenko, M. A. (2010). Loss of fish

Table S1. Lengths of the endoskeletal and AF regions

Stage (hpf)	Endoskeletal region (μm)	AF region (μm)	AF growth ratio (μm)
40	45.30	17.50	0.28
	61.20	20.30	0.25
	52.40	13.30	0.20
	41.40	14.80	0.26
	54.20	18.40	0.25
	47.30	20.40	0.30
Average (*n*=6)	50.30	17.50	0.26
45	127.07	43.86	0.26
	118.61	42.53	0.26
	123.52	38.71	0.24
	131.88	43.04	0.25
	124.52	46.44	0.27
	130.07	44.02	0.25
Average (*n*=6)	125.94	43.10	0.25
50	124.26	47.79	0.28
	105.78	47.46	0.31
	136.10	65.52	0.32
	114.82	67.73	0.37
	116.88	44.77	0.28
	116.27	37.22	0.24
Average (*n*=6)	119.02	51.75	0.30
55	107.63	38.49	0.26
	101.03	37.79	0.27
	102.95	45.60	0.31
	86.82	36.72	0.30
	149.02	97.17	0.39
	132.97	55.69	0.30
Average (*n*=6)	113.40	51.91	0.31
60	199.80	131.80	0.40
	150.37	108.37	0.42
	181.27	133.25	0.42
	161.07	102.93	0.39
	133.51	103.12	0.44
	137.19	91.80	0.40
Average (*n*=6)	160.54	111.88	0.41
70	226.24	156.87	0.41
	190.10	133.84	0.41
	203.75	144.18	0.41
	193.20	131.55	0.41
	204.53	125.60	0.38

	199.86	159.25	0.44
Average (*n*=6)	202.95	141.88	0.41
82	270.00	158.96	0.37
	233.63	148.22	0.39
	210.41	131.47	0.38
	243.08	145.64	0.37
	228.61	142.66	0.38
	198.71	151.77	0.43
Average (*n*=6)	230.74	146.45	0.39
92	243.08	190.99	0.44
	249.67	179.96	0.42
	215.72	166.21	0.44
	218.68	160.22	0.42
	232.63	179.20	0.44
	249.65	163.27	0.40
	227.04	171.57	0.43
Average (*n*=7)	233.78	173.06	0.43
104	234.92	184.99	0.44
	253.15	178.93	0.41
	233.54	176.25	0.43
	233.46	179.82	0.44
	238.20	181.11	0.43
	229.93	193.42	0.46
Average (*n*=6)	235.53	182.42	0.44
129	206.48	177.17	0.46
	209.62	178.45	0.46
	247.29	198.22	0.44
	247.72	189.84	0.43
	228.53	186.41	0.45
	238.04	204.78	0.46
	231.21	189.37	0.45
Average (*n*=7)	229.84	189.18	0.45

Endoskeletal and AF region lengths, measured in several stages of embryos from the same mating. Average values are graphed in Fig. 2H.

Table S2. Endoskeletal disc length after removing the apical fold (AF) (three times)

Sample	Control PD/AP lengths (μm)	Removal PD/AP lengths (μm)
1	245.4/184.2	239.9/182.1
2	252.6/174.3	282.2/173.6
3	271.9/170.7	303.7/158.3
4	249.8/168.8	299.7/189.2
5	229.2/162.3	259.5/151.0
6	228.4/168.5	266.2/174.3
7	240.0/166.9	334.7/164.0
Average	245.3/170.8	283.7/170.3

Values in this table represent one batch of experiments (n=7) and are displayed graphically in Fig. 6.

Table S3. Lengths of the endoskeletal and AF regions after treatment with SU5402 (Fgf inhibitor)

Sample	Control ed/AF lengths (μm)	SU5402 ed/AF lengths (μm)
1	195/121	130/95.9
2	180/119	82.0/88.2
3	208/139	136/83.4
4	235/128	106/102
5	241/139	115/108
6	232/142	108/92.1
7	206/125	111/95.7
8	215/140	135/98.4
9	176/134	96.9/115
10	201/135	96.1/70.0
11	215/138	124/107
12	199/148	
Average	208.6/134.0 (*n*=12)	112.7/95.97 (*n*=11)

Values in this table represent one batch of experiments and are displayed graphically in supplementary material Fig. S6E.
ed, endoskeletal region

Table S4. Lengths of the endoskeletal and AF regions in *tcf7* mutants

Sample	(hetero/control) ed/AF lengths (μm)	(homo) ed/AF lengths (μm)
1	244/151	192/60.4
2	195/141	163/86.0
3	217/143	195/94.2
4	232/140	197/132
5	202/156	223/127
6	182/131	145/96.8
7	214/139	170/98.4
8	222/145	179/101
9	179/143	195/93.6
10	172/142	
11	207/144	
12	185/140	
Average	204.3/142.9 (*n*=12)	184.3/98.8 (*n*=9)

Values in this table represent one batch of experiments and are displayed graphically in Fig. 8E.
ed, endoskeletal region